



## Soft magnetic properties and microstructure of $\text{Fe}_{84-x}\text{Nb}_2\text{B}_{14}\text{Cu}_x$ nanocrystalline alloys



Lin Xue<sup>a,b,c,d</sup>, Haishun Liu<sup>a,\*</sup>, Lintao Dou<sup>a</sup>, Weiming Yang<sup>a,b,c</sup>, Chuntao Chang<sup>b,c</sup>, Akihisa Inoue<sup>b,c</sup>, Xinmin Wang<sup>b,c</sup>, Run-Wei Li<sup>b,c</sup>, Baolong Shen<sup>d</sup>

<sup>a</sup> School of Sciences, China University of Mining and Technology, Xuzhou 221116, China

<sup>b</sup> Zhejiang Province Key Laboratory of Magnetic Materials and Application Technology, Ningbo Institute of Materials Technology & Engineering, Chinese Academy of Sciences, Ningbo 315201, China

<sup>c</sup> Key Laboratory of Magnetic Materials and Devices, Ningbo Institute of Materials Technology and Engineering, Chinese Academy of Sciences, Ningbo 315201, China

<sup>d</sup> School of Materials Science and Engineering, Southeast University, Nanjing 211189, China

### ARTICLE INFO

#### Article history:

Received 3 September 2013

Accepted 6 November 2013

Available online 15 November 2013

#### Keywords:

Nanocrystalline alloys

High saturation magnetization

Grain size

### ABSTRACT

Magnetic properties and microstructure of new  $\text{Fe}_{84-x}\text{Nb}_2\text{B}_{14}\text{Cu}_x$  nanocrystalline alloys were investigated. We found that the microstructure was refined and soft magnetic properties of this alloy system were enhanced with proper Cu addition and annealing conditions. It was also discovered that the mean grain size firstly increases, then decreases to a minimum, and finally increases again with increasing annealing temperature for  $\text{Fe}_{83}\text{Nb}_2\text{B}_{14}\text{Cu}_1$  nanocrystalline alloy, and this phenomenon was interpreted by the grain growth mechanism. Moreover, after annealing at 813 K for 180 s,  $\text{Fe}_{83}\text{Nb}_2\text{B}_{14}\text{Cu}_1$  nanocrystalline alloy shows a fine microstructure with mean grain size of 16 nm, and exhibits excellent soft magnetic properties, such as high saturation magnetic flux density (1.7 T), low coercivity (7 A/m) and high permeability ( $2.8 \times 10^4$ ). The result indicates that this alloy should have a promising application in the soft magnetic industry.

© 2013 Elsevier Ltd. All rights reserved.

### 1. Introduction

Fe-based nanocrystalline alloys, due to their excellent soft magnetic properties [1], have attracted great attention in physics [2–4], material science [5] as well as engineering application. They are widely used in soft magnetic components and devices, such as transformers, sensors, inductors and so on. In developing magnetic materials, two extreme cases are mostly of interest from an application point of view: one with the most excellent permeability and the other with the highest magnetic flux density [6]. So far, three famous kinds of Fe-based nanocrystalline alloys as Finemet [1], Nanoperm [7,8] and Hitperm [9] have been widely investigated experimentally [10–13] and theoretically [14–17]. Among these alloys, Nanoperm shows high saturation magnetic flux density (1.5–1.7 T) [18], high permeability ( $10^4$ ) [19], as well as small magnetostriction ( $\sim 0$  ppm) [20]. Therefore, it is favorable for toroidal cores, choke coils, power transformers, electro-magnetic interference, magnetic heads, and magnetic shielding [21,22]. However, the Nanoperm alloys generally contain relatively large amount (5–7 at.%) of expensive and easily oxidized elements (e.g. Zr or Hf), which limit its application to a certain extent [23,24]. Three

requirements should be met in order to obtain the Fe-based nanocrystalline alloy with not only excellent soft magnetic properties but also good productivity for industrial application [25]. The first is the formation of uniform nanostructure with small grain size and homogeneous distribution that is required to obtain good soft magnetic properties [26]. The second is a realization of the production of the alloy in air and low cost. Fe–Nb–B alloy with low Nb content less than 3 at.% was chosen to prevent the oxidation and lower the cost. The third is the achievement of high saturation magnetic flux density that requires high iron content. For above reasons, we focused on the new ternary  $\text{Fe}_{84}\text{Nb}_2\text{B}_{14}$  amorphous alloy containing as much as 84 at.% iron and only 2 at.% refractory Nb [27]. Therefore, the goal of this study is to realize the  $\text{Fe}_{84}\text{Nb}_2\text{B}_{14}$  based alloy with uniform microstructure and excellent soft magnetic properties as well. Additionally, Cu has a prominent effect on the formation of  $\alpha$ -Fe nanocrystals and the improvement of soft magnetic properties in Fe-based nanocrystalline alloys. It was found that Cu clustering occurs prior to the onset of crystallization, and the Cu clusters serve as heterogeneous nucleation sites for the primary crystallization of  $\alpha$ -Fe [28], which lead to a uniform microstructure.

In this paper, Cu in a range of 0–1.5 at.% was added to  $\text{Fe}_{84}\text{Nb}_2\text{B}_{14}$  alloy by a step of 0.25 at.%. Soft magnetic properties such as saturation magnetic flux density, coercivity, and

\* Corresponding author. Tel.: +86 139 12006872; fax: +86 516 83591591.

E-mail addresses: [liuhaishun@126.com](mailto:liuhaishun@126.com), [liuhaishun@cumt.edu.cn](mailto:liuhaishun@cumt.edu.cn) (H. Liu).

permeability were measured, the variation of grain size for nanocrystalline alloys, and their correlations with magnetic properties were also investigated.

## 2. Experimental details

Fe-based alloy ingots with nominal compositions of  $\text{Fe}_{84-x}\text{Nb}_2\text{B}_{14}\text{Cu}_x$  ( $x = 0.00, 0.25, 0.50, 0.75, 1.00, 1.25, 1.50$ ) were prepared by arc-melting a mixture of pure Fe (99.99%), Nb (99.99%), B (99.5%), and Cu (99.99%) under high purity argon atmosphere. Ribbons with a width of about 1 mm and thickness about 20–25  $\mu\text{m}$  were produced by single-roller melt spinning method. The crystallization temperature ( $T_x$ ) of as-quenched ribbons was measured by differential scanning calorimetry (DSC, NETZSCH 404C) with a heating rate of 0.67 K/s. Crystallization treatment was carried out by treating the as-quenched amorphous specimens at different temperatures for 180 s under vacuum followed by water quenching. Microstructure was examined by X-ray diffraction (XRD, Bruker D8 Advance) with Cu  $K\alpha$  radiation and transmission electronic microscopy (TEM, TECNAI F20), respectively. Saturation magnetic flux density ( $B_s$ ) and coercivity ( $H_c$ ) were measured with vibrating sample magnetometer (VSM, Lake shore 7410) under an applied field of 800 kA/m and DC B–H loop tracer (RIKEN BHS-40), respectively. Initial permeability ( $\mu_i$ ) in the frequency range of 1–101 kHz was measured with vector impedance analyzer (Agilent 4294A) under a field of 1 A/m.

## 3. Results and discussion

Fig. 1 shows XRD patterns taken from the free surface of the as-quenched ribbons for  $\text{Fe}_{84-x}\text{Nb}_2\text{B}_{14}\text{Cu}_x$  ( $x = 0–1.5$ ) alloys together with DSC curves. From the XRD patterns, it can be seen that alloys with proper copper additions ( $x = 0.50, 0.75,$  and  $1.00$ ) exhibit

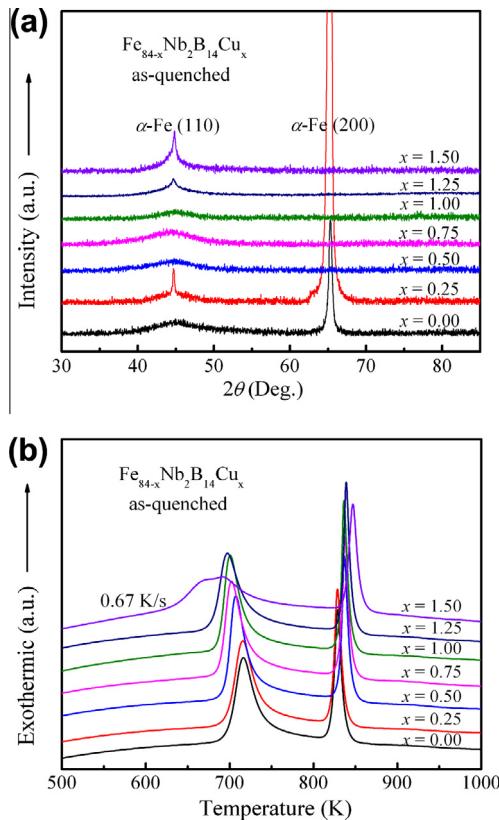


Fig. 1. XRD patterns and DSC curves of as-quenched  $\text{Fe}_{84-x}\text{Nb}_2\text{B}_{14}\text{Cu}_x$  alloys.

amorphous single phase. The DSC curves show that the crystallization of all these ribbons proceeds in two stages. The decrease of  $T_{x1}$  and the increase of  $T_{x2}$  with an increase of Cu content can be seen as well, thus enlarging the temperature interval ( $\Delta T_x = T_{x2} - T_{x1}$ ) between the two crystallization temperatures. This result indicates that Cu content seems to enhance the thermal stability of nanocrystallized alloy to a certain extent.

It can be found obviously in Fig. 2(a) that  $B_s$  rapidly increases from lower than 1.4 T to higher than 1.7 T as increasing annealing temperature ( $T_a$ ). This increase can be attributed to the appearance and growth of ferromagnetic crystalline grains of  $\alpha$ -Fe type phase embedded in the residual amorphous matrix and the increasing volume fraction of nanocrystalline phase with increasing annealing temperature. It can be seen from Fig. 2(b) that  $H_c$  decreases slightly at low temperatures and increases firstly to a high value, then decreases to a minimum and finally increases sharply to an even higher level for all the annealed alloys, while  $\mu_i$  changes in an opposite way as shown in Fig. 2(c). In the annealed  $\text{Fe}_{84-x}\text{Nb}_2\text{B}_{14}\text{Cu}_x$  alloys,  $H_c$  decreases with increasing addition of Cu at the optimal  $T_a$  between  $T_{x1}$  and  $T_{x2}$ , exhibiting a minimum  $H_c$  of 7 A/m and maximum  $\mu_i$  of  $2.8 \times 10^4$  at  $x = 1.00$ .

According to the random anisotropy model [29], the soft magnetic properties of nanocrystalline materials are ascribed to the averaging out of the magnetocrystalline anisotropy due to the random distribution of the anisotropy axis of the nanoscale grains. The  $H_c$  and  $\mu_i$  can be expressed as

$$H_c \approx p_c \frac{K_1^4 \cdot D^6}{J_s A^3} \quad (1)$$

$$\mu_i \approx p_\mu \frac{J_s^2 A^3}{\mu_0 K_1^4 \cdot D^6} \quad (2)$$

where  $A$  is the exchange stiffness,  $K_1$  the local magnetocrystalline anisotropy constant,  $J_s$  the saturation polarization,  $\mu_0$  the vacuum permeability,  $p_c$  and  $p_\mu$  dimensionless pre-factors of the order of

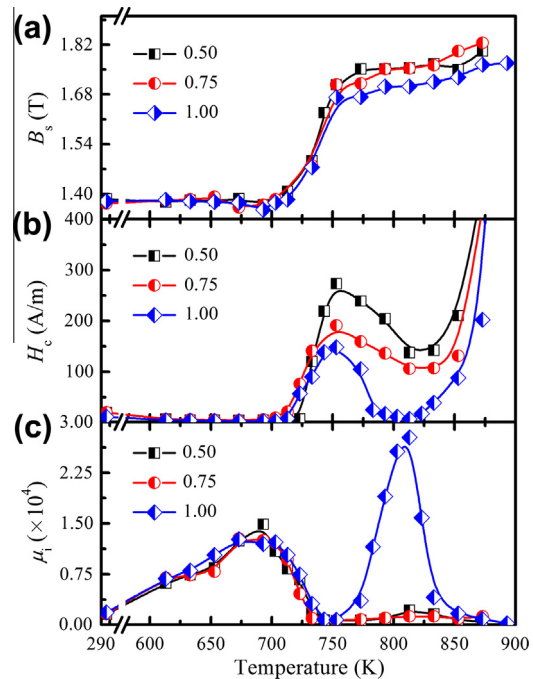
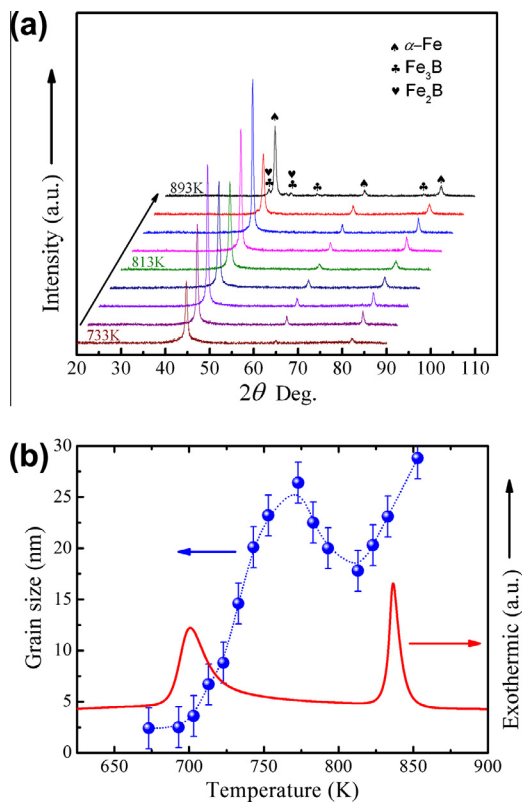


Fig. 2. Soft magnetic properties of annealed  $\text{Fe}_{84-x}\text{Nb}_2\text{B}_{14}\text{Cu}_x$  ( $x = 0.50, 0.75,$  and  $1.00$ ) alloys versus  $T_a$ . (a) Saturation magnetic flux density ( $B_s$ ), (b) coercivity ( $H_c$ ), and (c) initial permeability ( $\mu_i$ ). Lines for eye guide.

unity. From Eqs. (1) and (2), the coercivity and permeability were expected to roughly vary with grain size as  $H_c \propto D^6$  and  $\mu_i \propto 1/D^6$ , respectively. Therefore, the undulating changes in  $H_c$  and  $\mu_i$  are attributed to the variation of grain size  $D$  with increasing  $T_a$ .

Nanocrystals precipitated in the amorphous matrix were identified as  $\alpha$ -Fe phase after annealing at temperatures between  $T_{x1}$  and  $T_{x2}$  by XRD, as shown in Fig. 3(a). In order to confirm the above conjecture, grain sizes at different  $T_a$  were estimated from XRD patterns by Scherrer's equation. Fig. 3(b) shows the relationship between grain size and  $T_a$  for  $\text{Fe}_{83}\text{Nb}_2\text{B}_{14}\text{Cu}_1$  nanocrystalline alloy. The DSC curve of as-quenched  $\text{Fe}_{83}\text{Nb}_2\text{B}_{14}\text{Cu}_1$  alloy was also shown in Fig. 3(b) for comparison. It can be seen that the grain size firstly increases after  $T_{x1}$ , then decreases to a minimum between  $T_{x1}$  and  $T_{x2}$ , and finally increases again at higher temperatures. Furthermore, TEM was used to observe the microstructure of the annealed  $\text{Fe}_{83}\text{Nb}_2\text{B}_{14}\text{Cu}_1$  alloys for further investigation. It can be seen from the bright-field TEM images that nanoscale grains precipitate in all the examined samples while the grain sizes show an obvious difference. The bright-field images, selected area electron diffraction (SAED) patterns and grain size distributions of the alloys annealed for 180 s at 753 K, 813 K, and 873 K were shown in Fig. 4(a–c), respectively. The SAED patterns indicate that the  $\alpha$ -Fe nanocrystals [19] are randomly oriented in the annealed samples (inset in Fig. 4a–c). With optimum annealing temperature, uniform and fine  $\alpha$ -Fe grains can be seen in Fig. 4(b). In contrast, after annealing at lower temperature,  $\alpha$ -Fe with average grain size of about 25 nm can be seen sparsely distributed in the residual amorphous matrix, as shown in Fig. 4(a); after annealing at higher temperature, coarse  $\alpha$ -Fe with average grain size of about 30 nm can be seen in Fig. 4(c). Ring halo in Fig. 4(a) indicates the obvious residual amorphous phase in the sample, the low volume fraction of the nanocrystals at low annealing temperature was on account of the insufficient



**Fig. 3.** (a) XRD patterns of  $\text{Fe}_{83}\text{Nb}_2\text{B}_{14}\text{Cu}_1$  alloy after annealing at different temperatures. (b) Relationship between grain size and  $T_a$  of  $\text{Fe}_{83}\text{Nb}_2\text{B}_{14}\text{Cu}_1$  nanocrystalline alloy. DSC curve was also shown.

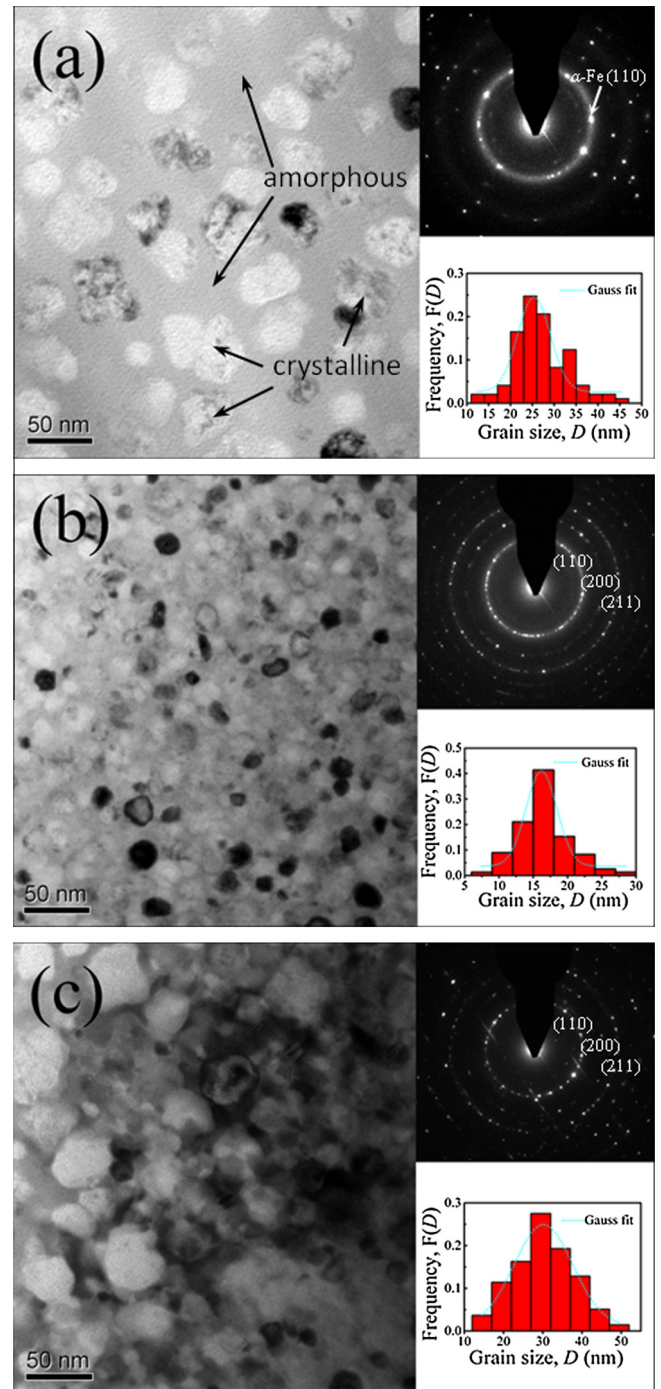


**Fig. 4.** Bright-field TEM, selected area diffraction pattern, and the distribution of gain size of the  $\text{Fe}_{83}\text{Nb}_2\text{B}_{14}\text{Cu}_1$  nanocrystalline alloy. (a) 753 K, (b) 813 K, and (c) 873 K. Blue dotted lines show Gaussian fitting. (For interpretation of the references to colour in this figure legend, the reader is referred to the web version of this article.)

nucleation sites and slow grain growth. To seek a precise description of grain size, the statistical analysis with respect to the grain size was carried out by analyzing more than 100 spots. By careful determination of the grain size in software Gatan Digital Microscopy Suite, it was found that the mean grain size of the composite of Fe–Nb–B–Cu with Fe nanograins annealed at 753 K, 813 K, and 873 K are 25.3 nm ( $\sigma = 6.21$ ), 16.2 nm ( $\sigma = 3.78$ ), and 30 nm ( $\sigma = 8.51$ ), respectively, which are consistent with the result estimated from XRD. The smaller standard deviation also indicates

the uniform microstructure of the nanocrystalline alloy annealed at 813 K. This phenomenon is consistent with previous research [30,31], and can be interpreted by the grain growth mechanism [32] of the coarsening of the pre-existing fine-crystalline structure to the nanocrystalline structure. The grain size is considered to be affected by two factors [33]: the nucleation rate and the grain growth rate. The growth rate increases with increasing temperature and the nucleation rate has a maximum at an intermediate temperature range where the minimum of the grain size arises. It is verified that the nucleation and crystal growth proceed at very fast rates near 813 K and the maximum of the nucleation rate may also occur at this temperature. Therefore, it is obvious that the microstructure with the smallest grain size can be formed only at about 813 K.

On the whole, Cu addition broadens the temperature interval ( $\Delta T_x = T_{x2} - T_{x1}$ ) between the two crystallization temperatures, favors the precipitation of  $\alpha$ -Fe, and inhibits the precipitation of other compounds [25,28,34]. With appropriate Cu addition ( $x = 1.00$ ) and annealing conditions, the composite of Fe–Nb–B–Cu with  $\alpha$ -Fe nanograins shows excellent soft magnetic properties. As the average grain size decreases from 25 nm to 16 nm and then increases to 30 nm, the  $H_c$  decreases from 140 A/m to 7 A/m and then increases to higher than 200 A/m, while  $\mu_i$  increases from  $1.8 \times 10^3$  to  $2.8 \times 10^4$  and then decreases to lower than  $2 \times 10^3$ , respectively. The high  $\mu_i$  is twice as large as that of the previous ternary Fe<sub>84</sub>Nb<sub>2</sub>B<sub>14</sub> alloy; and the high  $B_s$  up to 1.7 T is much higher than that of Fe<sub>84</sub>Nb<sub>2</sub>B<sub>14</sub> [27] and other existing Nanoperm-type alloy Fe<sub>84.9</sub>Nb<sub>6</sub>B<sub>8</sub>P<sub>1</sub>Cu<sub>0.1</sub> with more iron and high Nb content [25], which are 1.38 T and 1.61 T, respectively. Furthermore, the slight decrease of  $H_c$  was due to the release of internal stress in amorphous alloys at low  $T_a$  ( $T_a < T_{x1}$ ). When annealed at higher temperatures, it leads to the precipitation of iron–boride compounds like Fe<sub>2</sub>B or Fe<sub>3</sub>B, which are hard magnetic phases. Both the formation of Fe borides and grain coarsening significantly degrade the soft magnetic properties. Therefore,  $H_c$  decreases slightly at low temperatures, increases firstly to a high value for the coarse  $\alpha$ -Fe grains, then decreases to a minimum for the fine microstructure and finally increases sharply to an even higher level for the grain growth and the existence of iron–borides [11], while  $\mu_i$  has a reverse trend.

#### 4. Conclusions

In this work, Nb-poor Fe<sub>84-x</sub>Nb<sub>2</sub>B<sub>14</sub>Cu<sub>x</sub> nanocrystalline soft magnetic alloys with not only high saturation magnetic flux density but also lower cost were investigated. The results can be summarized as follows:

- (1) With appropriate Cu addition, Fe<sub>83</sub>Nb<sub>2</sub>B<sub>14</sub>Cu<sub>1</sub> nanocrystalline alloy obtained by annealing at 813 K for 180 s shows uniform microstructure and exhibits high saturation magnetic flux density (1.7 T), low coercivity (7 A/m), and high permeability ( $2.8 \times 10^4$ ).
- (2) The grain size of Fe<sub>83</sub>Nb<sub>2</sub>B<sub>14</sub>Cu<sub>1</sub> nanocrystalline alloy increases firstly after  $T_{x1}$  then decreases to a minimum for the refinement of the crystals and finally increases again. The undulating changes in  $H_c$  and  $\mu_i$  are attributed to the variation of grain size  $D$  with increasing  $T_a$ .

#### Acknowledgment

This work is supported by the Fundamental Research Funds for the Central Universities under Grant No. 2012LWB50.

#### References

- [1] Yoshizawa Y, Oguma S, Yamauchi K. New Fe-based soft magnetic alloys composed of ultrafine grain structure. *J Appl Phys* 1988;64:6044–6.
- [2] Sharma D, Chandra K, Misra PS. Design and development of powder processed Fe–P based alloys. *Mater Des* 2011;32:3198–204.
- [3] Shen TD, Schwarz RB, Thompson JD. Soft magnetism in mechanically alloyed nanocrystalline materials. *Phys Rev B* 2005;72:014431.
- [4] Suzuki K, Cadogan JM. Random magnetocrystalline anisotropy in two-phase nanocrystalline systems. *Phys Rev B* 1998;58:2730.
- [5] Stankov S, Yue YZ, Miglierini M, Sepiol B, Sergueev I, Chumakov AI, et al. Vibrational properties of nanograins and interfaces in nanocrystalline materials. *Phys Rev Lett* 2008;100:235503.
- [6] McHenry M, Laughlin D. Nano-scale materials development for future magnetic applications. *Acta Mater* 2000;48:223–38.
- [7] Suzuki K, Inoue A. Soft magnetic properties of bcc Fe–M–B–Cu (M = Ti, Nb or Ta) alloys with nanoscale grain size. *Jpn J Appl Phys* 1991;30:L1729–32.
- [8] Suzuki K, Makino A, Inoue A, Masumoto T. Soft magnetic properties of nanocrystalline bcc Fe–Zr–B and Fe–M–B–Cu (M = transition metal) alloys with high saturation magnetization. *J Appl Phys* 1991;70:6232–7.
- [9] Willard M, Laughlin D, McHenry M, Thoma D, Sickafus K, Cross JO, et al. Structure and magnetic properties of (FeCo) ZrBCu nanocrystalline alloys. *J Appl Phys* 1998;84:6773.
- [10] Kumar K, Swygenhoven HV, Suresh S. Mechanical behavior of nanocrystalline metals and alloys. *Acta Mater* 2003;51:5743–74.
- [11] Chen YM, Ohkubo T, Ohta M, Yoshizawa Y, Hono K. Three-dimensional atom probe study of Fe–B-based nanocrystalline soft magnetic materials. *Acta Mater* 2009;57:4463–72.
- [12] Gao Y, Shindo D, Bitoh T, Makino A. Mediated exchange interaction in Fe–Nb–B nanocrystalline soft magnetic materials. *Phys Rev B* 2003;67:172409.
- [13] Wang RW, Liu J, Wang Z, Gan ZH, Xiang ZD, Lu ZH, et al. Crystallization kinetics and magnetic properties of Fe<sub>63.5</sub>Co<sub>10</sub>Si<sub>13.5</sub>B<sub>9</sub>Cu<sub>1</sub>Nb<sub>3</sub> nanocrystalline powder cores. *J Non-Cryst Solids* 2012;358:200–3.
- [14] Herzer G. Grain-structure and magnetism of nanocrystalline ferromagnets. *IEEE Trans Magn* 1989;25:3327–9.
- [15] Herzer G. Modern soft magnets: amorphous and nanocrystalline materials. *Acta Mater* 2013;61:718–34.
- [16] Liu HS, Yin CH, Miao XX, Han ZD, Wang DH, Du YW. Soft magnetic properties and microstructure of novel Nb poor finemet type alloys. *Mater Sci Technol* 2008;24:45–8.
- [17] Yang WM, Liu HS, Dun CC, Zhao YC, Dou LM, Dou LT. Variations of the permeability with annealing conditions for Fe-based nanocrystalline alloys. *Mater Des* 2012;36:428–31.
- [18] Torrens-Serra J, Bruna P, Roth S, Rodriguez-Viejo J, Clavaguera-Mora M. Structural and magnetic characterization of Fe–Nb–B–Cu alloys as a function of Nb content. *J Phys D: Appl Phys* 2009;42:095010.
- [19] Torrens-Serra J, Peral I, Rodriguez-Viejo J, Clavaguera-Mora MT. Microstructure evolution and grain size distribution in nanocrystalline Fe–Nb–B–Cu from synchrotron XRD and TEM analysis. *J Non-Cryst Solids* 2012;358:107–13.
- [20] Hasiak M, Ciuzyńska W, Yamashiro Y, Fukunaga H. Soft magnetic properties of amorphous and nanocrystalline Fe<sub>80.7</sub>Zr<sub>4</sub>Ti<sub>3</sub>B<sub>12</sub>Cu<sub>1</sub> alloy. *J Magn Magn Mater* 2003;254:434–6.
- [21] Makino A, Inoue A, Masumoto T. Nanocrystalline Soft Magnetic Fe–M–B (M = Zr, Hf, Nb), “NANOPERM” Fe–M (M = Zr, Hf, Rare Earth) Alloys and Their Applications. *Materials Research Society Symposium Proceedings, Cambridge Univ Press* 1999; 457–468.
- [22] Naitoh Y, Bitoh T, Hatanai T, Makino A, Inoue A, Masumoto T. Applications of nanocrystalline soft magnetic Fe–MB (M = Zr, Nb) alloys. *Nanostruct Mater* 1997;8:987–95.
- [23] Friedrich J, Herr U, Samwer K. Early stages of mechanical crystallization of amorphous FeZrBCu soft magnetic material. *J Appl Phys* 2000;87:2464–8.
- [24] Torrens-Serra J, Roth S, Rodriguez-Viejo J, Clavaguera-Mora MT. Effect of Nb in the nanocrystallization and magnetic properties of Fe–Nb–B–Cu amorphous alloys. *J Non-Cryst Solids* 2008;354:5110–2.
- [25] Makino A, Bitoh T, Inoue A, Masumoto T. Nb-Poor Fe–Nb–B nanocrystalline soft magnetic alloys with small amount of P and Cu prepared by melt-spinning in air. *Scripta Mater* 2003;48:869–74.
- [26] Gao J, Li H, Jiao Z, Wu Y, Chen Y, Yu T, et al. Effects of nanocrystal formation on the soft magnetic properties of Fe-based bulk metallic glasses. *Appl Phys Lett* 2011;99:0525034–1–3.
- [27] Stokłosa Z, Rasek J, Kwapuliński P, Haneczok G, Chrobak A, Lełtko J, et al. Influence of boron content on crystallization and magnetic properties of ternary Fe–Nb–B amorphous alloys. *Phys Status Solidi A* 2010;207:452–6.
- [28] Hono K, Ping D, Ohnuma M, Onodera H. Cu clustering and Si partitioning in the early crystallization stage of an Fe<sub>73.5</sub>Si<sub>13.5</sub>B<sub>9</sub>Nb<sub>3</sub>Cu<sub>1</sub> amorphous alloy. *Acta Mater* 1999;47:997–1006.
- [29] Herzer G. Grain size dependence of coercivity and permeability in nanocrystalline ferromagnets. *IEEE Trans Magn* 1990;26:1397–402.
- [30] Hermann H, Mattern N, Roth S, Uebele P. Simulation of crystallization processes in amorphous iron-based alloys. *Phys Rev B* 1997;56:13888.
- [31] Zhang MX, Wang AD, Yang WM, Shen BL. Effect of Fe to P concentration ratio on structures, crystallization behavior, and magnetic properties in (Fe<sub>0.79+x</sub>P<sub>0.1-x</sub>C<sub>0.04</sub>B<sub>0.04</sub>Si<sub>0.03</sub>)<sub>99</sub>Cu<sub>1</sub> alloys. *J Appl Phys* 2013;113:17A337.

- [32] Yang WM, Liu HS, Dun CC, Zhao YC, Dou LM. Determine optimal annealing temperature of Fe based nanocrystalline alloys from their melting point. *Mater Sci Technol* 2012;28:1465–9.
- [33] Liu HS, Yang WM, Dun CC, Zhao YC, Dou LM. Unusual grain growth during annealing process: from amorphous to nanocrystalline. *Optoelectron Adv Mater-Rapid Commun* 2012;6:95–8.
- [34] Kong FL, Wang AD, Fan XD, Men H, Shen BL, Xie GQ, et al. High  $B_s$   $Fe_{84-x}Si_4B_8P_4Cu_x$  ( $x = 0-1.5$ ) nanocrystalline alloys with excellent magnetic softness. *J Appl Phys* 2011;109. 07A303–3.